



Microwave electromagnetic and absorption properties of SmN/ α -Fe/Sm₂Fe₁₇N₃ composites in 0.5–18 GHz range

Jinwen Ye, Ying Liu*, Xianfu Chen, Mingying Yao

School of Material Science and Engineering, Sichuan University, Chengdu 610065, China

ARTICLE INFO

Article history:

Received 27 September 2011
Received in revised form 13 February 2012
Accepted 17 February 2012
Available online xxx

Keywords:

Electromagnetic wave absorber
SmN/ α -Fe/Sm₂Fe₁₇N₃ composites
Complex permittivity and permeability

ABSTRACT

SmN/ α -Fe/Sm₂Fe₁₇N₃ composites were prepared in situ by heating of Sm₂Fe₁₇N₃ powders, and their electromagnetic wave absorption properties were measured in the frequency range of 0.5–18 GHz. The result shows that saturation magnetization and coercivity of as-heated powder with 23.7 wt% SmN, 58.5 wt% α -Fe and 17.8 wt% Sm₂Fe₁₇N₃ are 130.82 emu/g and 750 Oe, respectively. The dielectric constant of composites was low over the frequency range of 0.5–18 GHz, and their resonance frequencies were at a high frequency range. The effective electromagnetic wave absorption (RL < -20 dB) of the compact sample with thickness of 0.7–3.2 mm prepared with the SmN/ α -Fe/Sm₂Fe₁₇N₃ and resin was obtained in a frequency range of 5.5–16 GHz. A minimum reflection loss of -33 dB of the samples was observed at 5.5 GHz with an absorber thickness of 3.2 mm.

© 2012 Elsevier B.V. All rights reserved.

1. Introduction

Since Coey and Sun [1] discovered the interstitial compounds Sm₂Fe₁₇N_x, they have become one kind of the most promising modern hard magnetic materials, which exhibit outstanding magnetic properties. Unfortunately, because of their instability at temperatures above 500 °C, where they partly decompose into α -Fe and SmN, their magnetic properties are reduced and their applications are limited to be in the field of bonded magnets [2]. However, in these SmN/ α -Fe/Sm₂Fe₁₇N₃ composites, the hard magnetic Sm₂Fe₁₇N_x phase exhibits fairly large anisotropy field (14T), the soft magnetic α -Fe phase has high saturation magnetization (1.54T) [3] and the SmN phase can play a role as an insulating barrier to enhance the electrical resistivity of the composites [4]. According to the electromagnetic theory and existing reports on electromagnetic wave absorbers [5–7], natural resonance frequency f_r of these SmN/ α -Fe/Sm₂Fe₁₇N₃ composites should be at a higher frequency range and so their relative complex permeability μ_r should remain in high values at the frequency range. So, it is possible to make thinner absorbers in a higher frequency range from SmN/ α -Fe/Sm₂Fe₁₇N₃ composites than those prepared with the ferrites. Furthermore, the resistivity values of these composites may be higher than that of the metallic soft magnetic materials as well [8]. Therefore, SmN/ α -Fe/Sm₂Fe₁₇N₃ composites are potential to become a new type of thinner electromagnetic wave absorbers at the high frequency range. However, concerning the

preparation and properties of the SmN/ α -Fe/Sm₂Fe₁₇N₃ composites as the microwave electromagnetic absorbers, basic data are still lacking. In this paper, microstructure, microwave electromagnetic and absorption properties of the SmN/ α -Fe/Sm₂Fe₁₇N₃ composites during the frequency range of 0.5–18 GHz were investigated.

2. Experimental

The SmN/ α -Fe/Sm₂Fe₁₇N₃ composites were prepared in situ by heating of Sm₂Fe₁₇N₃ powders at above 750 °C for 10 min in a vacuum furnace. The heated Sm₂Fe₁₇N₃ powders were pulverized for 25 h using a planetary ball milling machine. X-ray diffraction (XRD) measurements were performed using a DX-2000 X-ray diffraction tester with Cu K α radiation by a step scanning method radiation with a 2θ range from 19° to 90°, step 0.02°, time 15 s. Qualitative and quantitative analyses were carried by the Rietveld method using Jade programmer. Scanning electron microscope (SEM) and high resolution transmission electron microscope (HRTEM) were adopted to determine the microstructure of the samples. The magnetic hysteresis loops were measured using a vibrating sample magnetometer (Lakeshore VSM 7410). A powder mixture was obtained with 83 wt% Sm₂Fe₁₇N₃ powders and 17 wt% paraffin. Then the powder mixture was compacted into samples in toroidal shape (7.00 mm outer diameter, 3.04 mm inner diameter and approximately 3 mm thickness.) and rectangular shape (L \times W = 7.2 \times 3.6: corresponding to the size of various wave guide, thickness: 0.9 mm). The vector value of reflection/transmission coefficient (scattering parameters) of the samples were measured in the frequency range of 0.5–18 GHz, using an Agilent 8720ET vector network analyzer. The relative permeability (μ_r) and permittivity (ϵ_r) values were determined from the scattering parameters and sample thickness. Assumed that the metal material was underlay of the absorber, the reflection loss (RL) curves were calculated from the relative complex permeability values and the permittivity values at a given frequency range and a given absorber thickness (d), the following equations were presented [9]:

$$RL = 20 \log \left| \frac{Z_{in} - 1}{Z_{in} + 1} \right| \quad (1)$$

$$Z_{in} = \text{sqr} \left(\frac{\mu_r}{\epsilon_r} \right) \tanh \left\{ j \frac{2\pi f d}{c} \text{sqr}(\mu_r \epsilon_r) \right\} \quad (2)$$

* Corresponding author Tel.: +86 2885405332; fax: +86 2885405332.
E-mail address: liuying5536@163.com (Y. Liu).

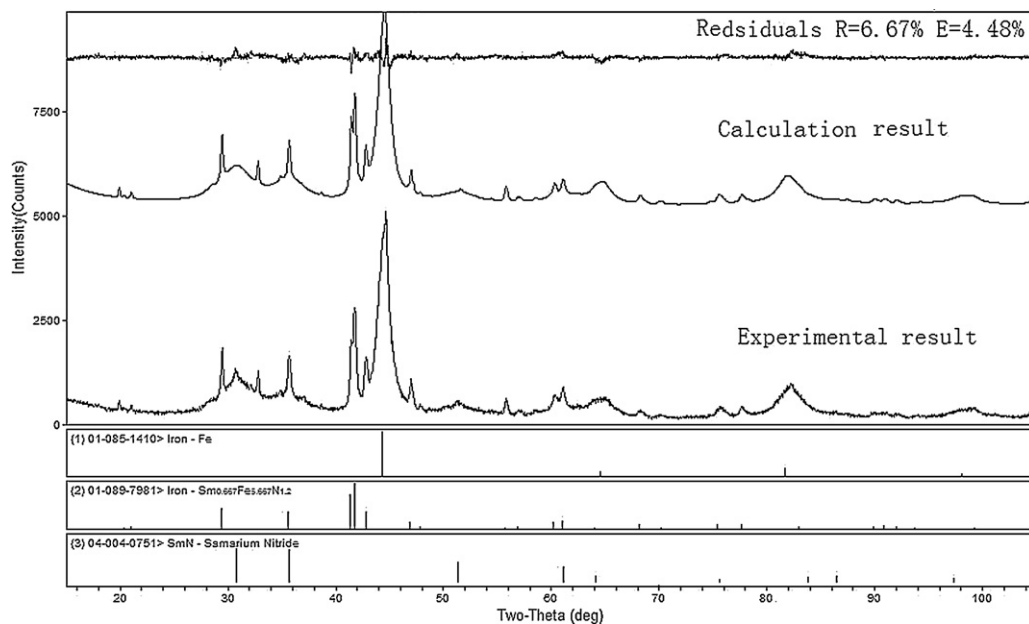


Fig. 1. XRD patterns of the as-heated $\text{Sm}_2\text{Fe}_{17}\text{N}_3$ powders (a) and calculation result by the Rietveld method (b).

where Z_{in} is the normalized input impedance at absorber surface, f is the frequency of microwave, and c is the velocity of light.

3. Results and discussion

The XRD patterns of as-heated $\text{Sm}_2\text{Fe}_{17}\text{N}_3$ powders are showed in Fig. 1. In our previous study [10], the reflections in $\text{Sm}_2\text{Fe}_{17}\text{N}_3$ powders (before heated) can be attributed to $\text{Sm}_2\text{Fe}_{17}\text{N}_3$ phase with a rhombohedral $\text{Th}_2\text{Zn}_{17}$ -type structure, co-existing with neglectable α -Fe phases, and SmN phase is undetectable. From Fig. 1, it is confirmed that $\text{Sm}_2\text{Fe}_{17}\text{N}_3$ powders partly decomposed into SmN and α -Fe, and the heated powder is a three-phase mixture of 58.5 wt% α -Fe, 23.7 wt% SmN and 17.8 wt% $\text{Sm}_2\text{Fe}_{17}\text{N}_3$ (calculated by Rietveld Method, Residuals $R=6.67\%$, $E=4.48\%$). Fig. 2 shows the SEM images of the heated $\text{Sm}_2\text{Fe}_{17}\text{N}_3$ powders before and after ball-milling. For as-heated $\text{Sm}_2\text{Fe}_{17}\text{N}_3$ powders (Fig. 2(a)), the particle size distribution is 5–10 μm , with increasing the ball-milling time to 25 h, it is decreased to about 2–5 μm and finally flakes-like powders (Fig. 2 (b)) are obtained, which are favorable to enhance the absorbing ability of the material. For more detailed discussions, transmission electron microscope (TEM) observations for these composites powders are given in Fig. 3. It is quite evident that SmN phase and undecomposed $\text{Sm}_2\text{Fe}_{17}\text{N}_3$ phase dispersed in

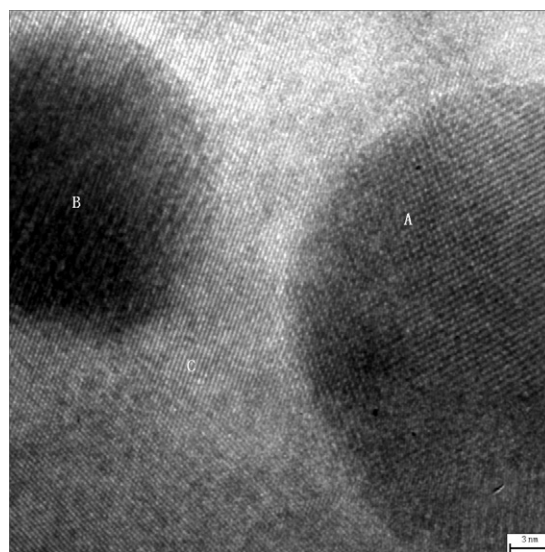


Fig. 3. HRTEM micrograph of the as-heated $\text{Sm}_2\text{Fe}_{17}\text{N}_3$ powders, (A) $\text{Sm}_2\text{Fe}_{17}\text{N}_3(003)$, (B) SmN (111), (C) α -Fe (110).

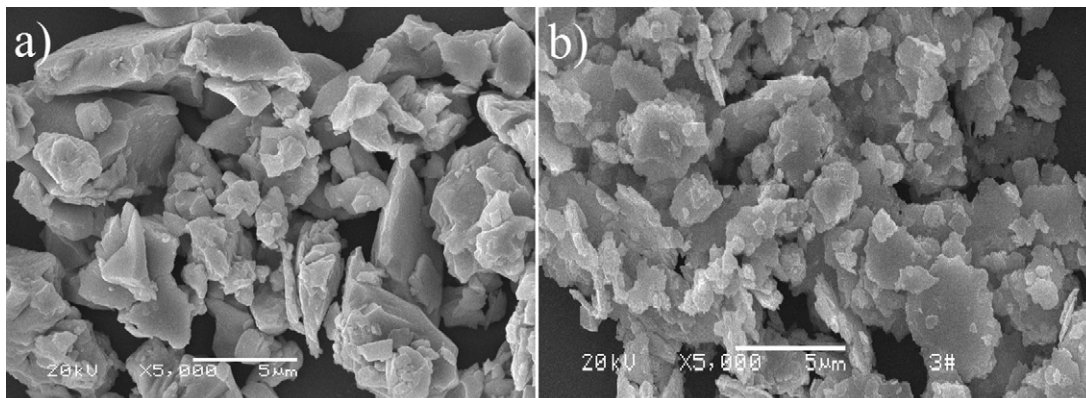


Fig. 2. SEM images of the as-heated $\text{Sm}_2\text{Fe}_{17}\text{N}_3$ powders before (a) and after (b) ball-milling.

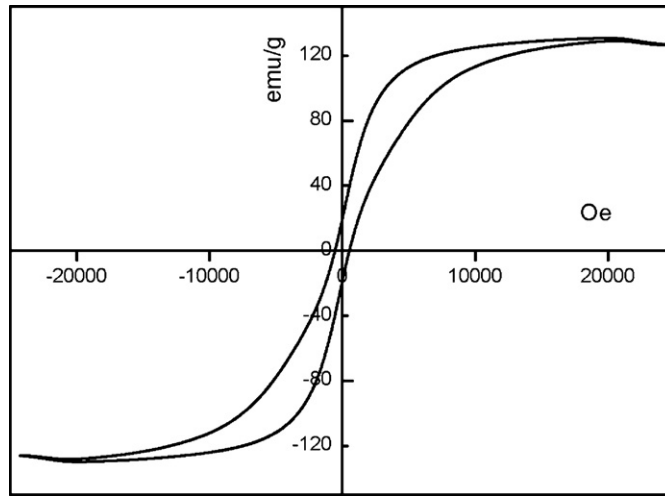


Fig. 4. Magnetic hysteresis loop for SmN/α-Fe/Sm₂Fe₁₇N₃ composites.

the α-Fe matrix phase, and there is disorder structure in the grain boundaries of α-Fe phase. As shown in Fig. 3, cross (003) lattice fringes of Sm₂Fe₁₇N₃ phase with $a=0.42$ nm (see grains A), (111) lattice fringes of SmN phase with $a=0.29$ nm (see grains B) and (110) lattice fringes of α-Fe phase with $a=0.20$ nm (see grains C) are observed.

Fig. 4 is a magnetic hysteresis loop for the prepared SmN/α-Fe/Sm₂Fe₁₇N₃ composites. From Fig. 4, it can be seen that values of saturation magnetization (M_s) and coercivity (H_c) are 130.82 emu/g and 750 Oe, respectively, which are rather higher than those of common soft magnetic materials such as the hexaferrite-FeCo nanocomposite [8]. Furthermore, the magnetic

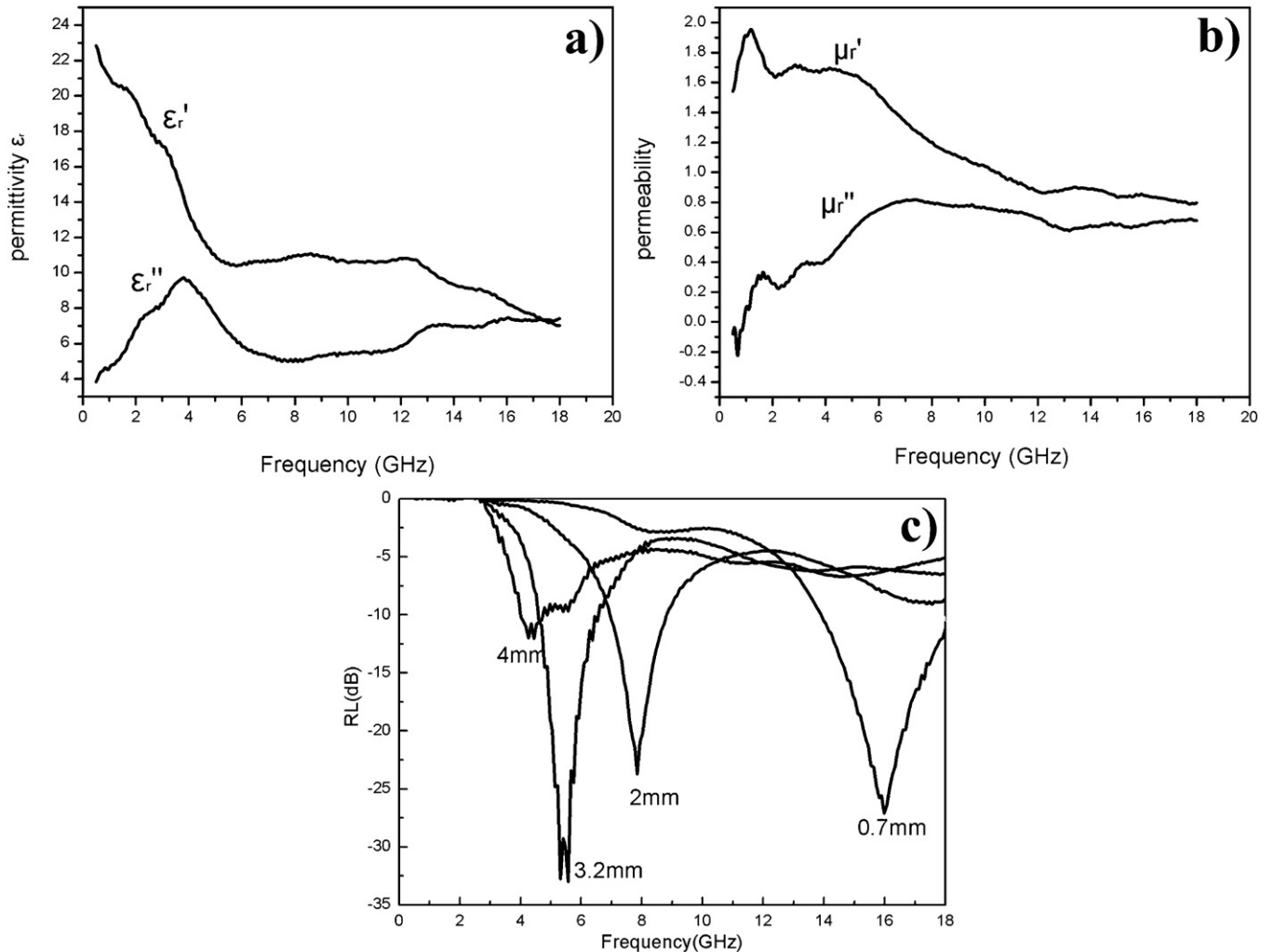


Fig. 5. Frequency dependences of relative permittivity ϵ_r (a), permeability μ_r (b) and RL (c) for the resin of SmN/α-Fe/Sm₂Fe₁₇N₃ composites.

hysteresis loops are quite smooth, which shows the characteristics of a single phase hard magnetic material. This result can be explained by the effect of exchange interaction between the hard magnetic $\text{Sm}_2\text{Fe}_{17}\text{N}_3$ and soft magnetic $\alpha\text{-Fe}$ [7]. Compared with conventional ferrite materials, the $\text{SmN}/\alpha\text{-Fe}/\text{Sm}_2\text{Fe}_{17}\text{N}_3$ magnetic materials have larger saturation magnetization value and their Snoek limit is at 50–60 GHz. These lead to the value of relative complex permeability of the composites remain rather high in a higher frequency range.

The complex relative permeability and permittivity for $\text{SmN}/\alpha\text{-Fe}/\text{Sm}_2\text{Fe}_{17}\text{N}_3$ magnetic materials in the frequency range of 0.5–18 GHz are shown in Fig. 5. As can be clearly seen, the real part ε_r' decreases with increasing frequency for $\text{SmN}/\alpha\text{-Fe}/\text{Sm}_2\text{Fe}_{17}\text{N}_3$ composites in 0.5–18 GHz, however the imaginary part ε_r'' exhibits a peak at 3.8 GHz. The dielectric constant of $\text{SmN}/\alpha\text{-Fe}/\text{Sm}_2\text{Fe}_{17}\text{N}_3$ composites is lower than that of metallic soft magnetic materials [4] due to the high resistance of SmN phase, and the disorder structure around $\alpha\text{-Fe}$, which is good to reducing eddy currents and satisfying the requirement of impedance matching. The permeability spectra of $\text{SmN}/\alpha\text{-Fe}/\text{Sm}_2\text{Fe}_{17}\text{N}_3$ composites shows relaxation and multi-peak resonant type characteristic in the 0.5–18 GHz frequency ranges, as shown in Fig. 5(b). The real part μ_r' is increased from about 1.54 to 2.0 in the 0.5–1.2 GHz range and then decreased with increase of frequency. Nevertheless, the imaginary part μ_r'' increased from -0.09 to 0.85 in the 0.05–6.0 GHz range, and broad peaks with about maximum values at different frequencies between 6–13 GHz were observed, then increased in the higher-frequency range. The high permeability in the samples is ascribed to 17.8 wt% hard magnetic $\text{Sm}_2\text{Fe}_{17}\text{N}_x$ phase, and their exchange interaction with soft magnetic $\alpha\text{-Fe}$ phase, also a reduction in eddy current losses due to micro-grain size (see Fig. 2 and Fig. 3) and the high resistance of the powder.

It is well known that the ferromagnetic resonance frequency f_r is related to its anisotropy field H_a by the following relation:

$$2\pi f_r = rH_a \quad (3)$$

where r is the gyromagnetic ratio. $\text{SmN}/\alpha\text{-Fe}/\text{Sm}_2\text{Fe}_{17}\text{N}_3$ composites have a larger anisotropy field H_a than $\alpha\text{-Fe}$ phase (judging from the hysteresis loop in Fig. 4), and consequently their natural resonance frequency f_r is at a high frequency range, according to the Formula (3). This sample exhibits a maximum μ_r'' value of 0.85 at 6 GHz, which is higher than those of $\alpha\text{-Fe}$, 1.6 GHz. Thus the observed resonance phenomena in Fig. 5(b) can be attributed to the resistance to the spin rotation. In addition, the ferromagnetic resonance plays an important role in the high frequency region. The frequency dependence of resulting RL values for the resin composite of $\text{SmN}/\alpha\text{-Fe}/\text{Sm}_2\text{Fe}_{17}\text{N}_3$ powders is showed in Fig. 5(c). This composite realized the optimum matching reflection loss $\text{RL} < -20$ dB in the 5.5–16 GHz range with an absorber thickness between 0.7 and 3.2 mm. Particularly, a minimum RL of -33 dB was obtained at

5.5 GHz with a thickness of 3.2 mm and the minimum d_m value of 0.7 mm is obtained at 16 GHz with a 1.6 GHz bandwidth for RL less than -20 dB. Consequently, efficient EM absorption properties of the $\text{SmN}/\alpha\text{-Fe}/\text{Sm}_2\text{Fe}_{17}\text{N}_3$ composites are observed in 0.5–18 GHz with high frequency range, in good impedance matching and thickness of absorber.

4. Conclusions

In conclusion, $\text{SmN}/\alpha\text{-Fe}/\text{Sm}_2\text{Fe}_{17}\text{N}_3$ composites were successfully prepared in situ by heating of $\text{Sm}_2\text{Fe}_{17}\text{N}_3$ powders at above 750°C for 20 min in a vacuum furnace and pulverized by ball milling. The dielectric constant of the composites is low due to high resistance of SmN phase and the disorder structure around $\alpha\text{-Fe}$ structure. The real part μ_r' is decreased from 2.0 to 0.8 with frequency and imaginary part μ_r'' exhibited wide peaks with about maximum values at different frequencies between 6–13 GHz owing to their high magnetocrystalline anisotropy field H_a values. A resin compacts of $\text{SmN}/\alpha\text{-Fe}/\text{Sm}_2\text{Fe}_{17}\text{N}_3$ powders provided good electromagnetic microwave absorption performances reflection loss < -20 dB in the range of 5.5–16 GHz with an absorber thickness between 0.7 and 3.2 mm, which demonstrate that the $\text{SmN}/\alpha\text{-Fe}/\text{Sm}_2\text{Fe}_{17}\text{N}_3$ composites are promising for the application to produce thin and light wave absorbers.

Acknowledgments

This work was supported by Doctoral Fund for New Teachers no. 200806101020 from the Ministry of Education China and the National Natural Science Foundation of China (Grant no. 51104103).

References

- [1] J.M.D. Coey, H. Sun, J. Magn. Magn. Mater. 87 (1990) L251.
- [2] T. Iriyama, K. Kobayashi, N. Imaoka, T. Fukuda, H. Kato, Y. Nakagawa, IEEE Trans. Magn. 28 (5.) (1992) 2326–2331.
- [3] Shandong Li, Ming Liu, Feng Xu, J. Lou, Zongjun Tian, Jianpeng Wu, Yi Hu, Xinle Cai, J.-G. Duh, N.X. Sun, J. Appl. Phys. 109 (2011) 07A315.
- [4] Guozhi Xie, Ping. Wang, Baoshan Zhang, Liukui Yuan, Yi. Shi, Pinghua Lin, Huaixian Lu, J. Magn. Magn. Mater. 320 (2008) 1026–1029.
- [5] J.-r. Liu, Masahiro Itoh, Masao Terada, Takashi Horikawa, K.-i. Machida, Appl. Phys. Lett. 91 (2007) 093101.
- [6] Koji Miura, Masahiro Masuda, Masahiro Itoh, Takashi Horikawa, K.-i. Machida, J. Alloys Compd. 408–412 (2006) 1391–1395.
- [7] Sugimoto, T. Maeda, D. Book, T. Kagotani, K. Inomata, M. Homma, H. Ota, Y. Houjou, R. Sato, J. Alloys Compd. 330–332 (2002) 301–306.
- [8] Li-X. Lian, L.J. Deng, M. Han, W. Tang, S.-D. Feng, J. Alloys Compd. 441 (2007) 301–304.
- [9] F.S. Ma, H.S. Lim, Z.K. Wang, S.N. Piramanayagam, S.C. Ng, M.H. Kuok, Appl. Phys. Lett. 98 (2011) 153107.
- [10] Jinwen Ye, Ying Liu, Guoli Zhu, Mei Chen, Shengji Gao, Mingjing Tu, J. Alloys Compd. 428 (2007) 350–354.